LANGMUIR

Article

pubs.acs.org/Langmuir

Yolk/Shell Colloidal Crystals Incorporating Movable Cores with Their Motion Controlled by an External Electric Field

Kanako Watanabe,[†] Haruyuki Ishii,[†] Mikio Konno,[†] Arnout Imhof,[‡] Alfons van Blaaderen,[‡] and Daisuke Nagao*[,†]

[†]Department of Chemical Engineering, Tohoku University, 6-6-07 Aoba, Aramaki-aza Aoba-ku, Sendai 980-8579, Japan

[‡]Soft Condensed Matter, Debye Institute for Nanomaterials Science, Utrecht University, Princetonplein 5, 3584 CC Utrecht, The Netherlands

Supporting Information

ABSTRACT: Yolk/shell particles composed of a submicrometer-sized movable core and a silica shell are promising building blocks for novel optical colloidal crystals, because the locations of cores in the shell compartment can be reversibly changed by using external stimuli. Two dimensional arrays of yolk/shell particles incorporating movable cores were prepared by a self-assembly method. The movable cores of colloidal crystals in water could be observed with an optical microscope under application of external electric field. The motions of inner silica cores depended on the electric field strength and frequency and were categorized into three cases: (1) Random Brownian motion, (2) anisotropic motion of cores moving in a direction orthogonal to a field, and (3) suppressed motion fixed in the center of shell compartment. Random Brownian motion of cores was scarcely affected by field strength when a high frequency (in the MHz range) electric field was applied. On the other hand, an increase in field strength at low-frequency fields (kHz) transiently changed the core motion from (1) to (2) and a further increase in field strength changed it from (2) to (3). When the silica core was incorporated in a large void a stronger electric field was needed to suppress its motion than when it was in a small void. The high responsivity to electric fields in a low-frequency range indicated the importance of electric double layer (EDL) interaction between core and inner shell in controlling the core location in yolk/shell colloidal crystals. It was also shown that movable titania cores in yolk/shell particles required a low-frequency field with a high strength to change from the random to anisotropic motion. The result suggested that the electrostatic interaction between EDLs of the silica core and the inner silica wall could be stronger than that between EDLs of the titania core and the silica shell.

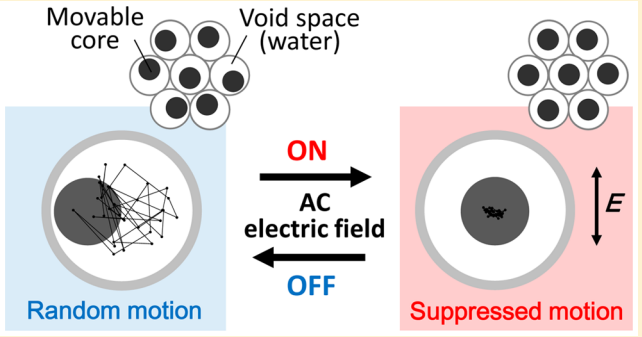

INTRODUCTION

Colloidal crystals composed of complex building blocks are promising materials for optical,[1,2] electrical,[3] and biomedical applications.[4] Creation of soft materials constituted of building blocks at changeable distances is an effective way for tuning their optical or electrical properties with external stimuli. Their creation will diversify their applications as chemical[5] or biological sensors,[6] displays,[7,8] and printings.[9,10] To control the relative distance between building blocks, for instance, thermosensitive polymers such as poly(*N*-isopropylacrylamide) have been employed as colloidal crystal matrices for tuning their optical properties by temperature-induced phase transition of the polymers.[11,12] Application of external fields such as electric and magnetic fields has also been employed to gain control over arrangements of building blocks in the formation of colloidal crystals. Typical examples of using external fields are electro- or magnetorheological fluids in which building blocks are assembled into ordered or nonordered chain structures due to dipolar interactions between the building blocks.[13,14] In the systems reported, however, the reconfiguration[15−19] or volume phase transitions[11,12] of building blocks were required to switch their locations in the assembled structure.

Yolk/shell colloidal crystals are promising materials for switchable optical properties without reconfiguration or volume transitions. A previous report[20] on calculation with a plane-wave-based transfer-matrix method showed an intriguing optical property of yolk/shell colloidal crystals containing movable magnetic cores. It was expected in the calculation that the stop bands of the colloidal crystals could be changed by controlling the location of inner cores with external magnetic fields.

We have recently reported a novel type of colloidal crystals comprising yolk/shell particles incorporating a movable core the location of which can be magnetically controlled.[21] In our colloidal crystals, where the micrometer-sized yolk/shell

Received: August 23, 2016
Revised: November 15, 2016
Published: December 12, 2016

DOI: 10.1021/acs.langmuir.6b03116
Langmuir 2017, 33, 296−302

particles were two-dimensionally assembled into hexagonal structures, application of a magnetic field could rearrange the locations of movable cores without a significant change in the relative locations of the silica shells.

An external electric field may also be usable to switch the motion and location of the cores in colloidal crystals of yolk/shell particles. Various structures of the cores in the shell compartment would be obtainable by controlling field strengths and frequencies.

The purpose of the present work is twofold: one is to fabricate two-dimensional yolk/shell particle arrays incorporating movable cores that are responsive to an external electric field. Submicrometer-sized cores of the yolk/shell particles are chosen as they are of interest for future application as optical devices employing visible light. The other one is to explore the application conditions of electric fields to control the motions and locations of cores in the shell compartment.

EXPERIMENTAL SECTION

Materials. Tetraethyl orthosilicate (TEOS, 95%), titanium tetraisopropoxide (TTIP, 95%), acetonitrile (99.5%), ammonia aqueous solution (25 wt %), methylamine aqueous solution (40 wt %), ethanol (99.5%), styrene (St, 99%), *p*-styrenesulfonic acid sodium salt (NaSS, 80%), and potassium persulfate (KPS, 95.0%) were purchased from Wako Pure Chemical Industries (Osaka, Japan). 3-Methacryloxypropyltrimethoxysilane (MPTMS, 95.0%) was obtained from Shinetu Chemical (Tokyo, Japan). The inhibitor for St monomer was removed by using an inhibitor removal column. Polyvinylpyrrolidone (PVP, M_W = 360 000 g/mol) was purchased from Tokyo Chemical Industry. Poly(allylamine hydrochloride) (PAH, M_W = 15 000 g/mol) was obtained from Aldrich. The silane coupling agent 3-aminopropyltrimethoxysilane (APTES, 95%) was purchased from Chisso Corp (Tokyo, Japan).

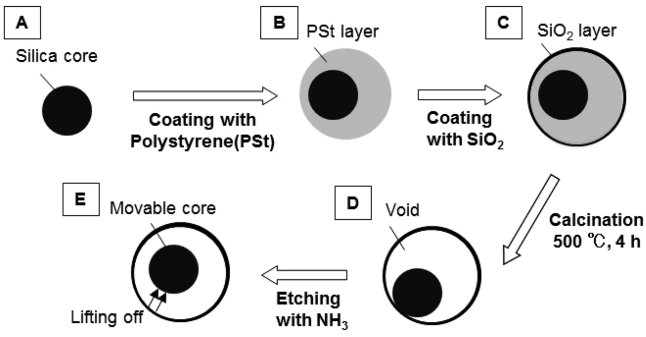

Figure 1. Schematic procedure of yolk/shell particles incorporating a silica core.

Synthetic Procedure. *Yolk/Shell Particles Incorporating a Silica Core.* Figure 1 shows the schematic procedure for preparation of yolk/shell particles. The submicrometer-sized silica cores shown in Figure 1A were prepared according to our method previously reported.[22]

The silica cores were surface-modified with MPTMS (2 mM) for a silica core concentration of 0.15 vol % (in deionized water) at 35 °C. To a suspension of the surface-modified cores, St (50 mM) and an aqueous solution of NaSS were added. After stirring for 30 min at 65 °C, an aqueous solution of KPS was added to the suspension as an initiator. Formation of a PSt shell was conducted at [KPS] = 2 mM, [NaSS] = 0.25 mM, and a silica concentration of 0.15 vol %. To further increase the thickness of the PSt shell, another polymerization of St was conducted at a concentration of 100 mM or 200 mM with KPS initiator (2 mM). The second formation of PSt shell was performed at a core/shell particle concentration of 0.05 vol %.

In the second step (Figure 1B → C), the doubly PSt-coated silica particles were coated with silica.[23] A suspension of the PSt-coated particles was added to a solution containing PAH and NaCl. The concentrations of the doubly PSt-coated particles, PAH, and NaCl were 0.15 vol %, 0.71 kg/m^3, and 36 mol/m^3 in the mixture, respectively. After two centrifugation steps to remove nonadsorbed PAH and NaCl, the particles were redispersed into 40 mL of an ethanolic solution containing 0.20 g of polyvinylpyrrolidone (PVP). Two more centrifugation steps were conducted to remove excess PVP, and particles were redispersed into 9.59 mL of ethanol. To the ethanolic solution, 10.6 mL of ammonia solution, silica precursors TEOS (1 mL) and APTES (37 μL) were added. The mixed silica precursors were used to form a low-density silica shell suitable for the slight etching of silica in the Figure 1D → E step.[24,25]

PSt particles coated with silica were dried at 50 °C, followed by heat treatment for 4 h in air in an oven at 500 °C (Figure 1C → D). Particles obtained by the heat treatment were immersed in 30 mL of ammonia solution (15−20 mM, approximately pH 11) to slightly etch the silica component of the particles (Figure 1D → E). This detaches the cores from the shells.

Yolk/Shell Particles Incorporating a Titania Core. The yolk/shell particles were prepared with almost the same method as the yolk/shell particles incorporating a silica core. Submicrometer-sized titania cores were prepared according to our method previously reported.[26,27] The titania cores were surface-modified with MPTMS at 35 °C. After an hour reaction under stirring, styrene monomer (50 mM) and an aqueous solution of NaSS were added to the suspension and the mixture was stirred for 1 h. An aqueous solution of KPS was added as an initiator to the suspension at 65 °C. The polymerization was conducted at [MPTMS] = 2 mM, [KPS] = 2 mM, [NaSS] = 0.25 mM, and a titania concentration of 0.065 vol %.

Preparation of Yolk/Shell Particle Assembly. Two-dimensional assemblies of the yolk/shell particles were prepared with the facile method previously reported.[28] A cover glass (Matsunami Glass, Φ = 18 mm) on which a small amount of suspension (15 μL) was dropped was dried for 6 h or more. Prior to this, the cover glass was hydrophilized by UV ozone irradiation for 1 h (Biosource Nanosciences, UV/ozone Procleaner, PC450). The particle concentration in the suspension was 1 wt %.

Characterization. The yolk/shell particles were observed with FE-TEM (Hitachi, HD-2700). An external AC field was applied to the particle assembly in deionized water with a function generator (GWINTEK, SFG-2004) and amplifier (NF Circuit Design Bloc, HSA4011). The electric field strengths and frequencies are summarized in Table 1. The electric field strength (peak to peak) was measured with a digital oscilloscope (GWINTEK, GDS-1062A). Schematic procedure for fabrication of the set up to apply an electric field is shown in Figure S1. The inner cores with and without applied field were observed with an optical microscope (Nikon, C2$_{Si}$) under 150× magnification in an area of 51.20 × 40.96 μm^2. The motion of cores was analyzed by a tracking system (Nikon, NIS-A Object Tracking) that can trace cores within an error of 40 nm corresponding to 1 pixel.

RESULTS AND DISCUSSION

As described in the Experimental Section, yolk/shell particles to be used as building blocks for two-dimensional arrays were synthesized in the route of Figure 1. Silica cores with an average size of 372 nm (C_V = 3.6%) comparable to visible light wavelengths were prepared with a sol−gel method. The core−shell particles (Figure 1B) were formed in soap-free emulsion polymerization in the presence of silica particles surface-modified with 3-methacryloxypropyltrimethoxysilane, and the silica-coated core−shell particles (Figure 1C) were heated at 500 °C for 4 h to remove the polymer component from the silica-coated particles. Figure 2a shows a TEM image of particles obtained by immersing the yolk−shell particles in a slightly basic solution of ammonia (15−20 mM, approximately pH 11). The alkaline etching process rendered the silica shell more porous and thinner than the particles before etching

DOI: 10.1021/acs.langmuir.6b03116
Langmuir 2017, 33, 296−302

Table 1. Dependences of Core Motions on Field Strength and Frequency

		motions of inner cores[a]		
		SiO_2 core		TiO_2 core
frequencies	electric field strengths	d_{void}/d_{core} = 3.0	d_{void}/d_{core} = 2.2	d_{void}/d_{core} = 2.2
0.5 kHz	0 V/mm	R	R	R
	50 V/mm	A	A	R
	100 V/mm	A	S	A
	150 V/mm	S	S	A
1 kHz	0 V/mm	R	R	R
	50 V/mm	A	A	R
	100 V/mm	A	S	A
	150 V/mm	A	S	A
1 MHz	0—150 V/mm	R	R	R

[a]A, anisotropic; S, suppressed; R, random Brownian motion. The definitions of the sizes are shown in Figure S2.

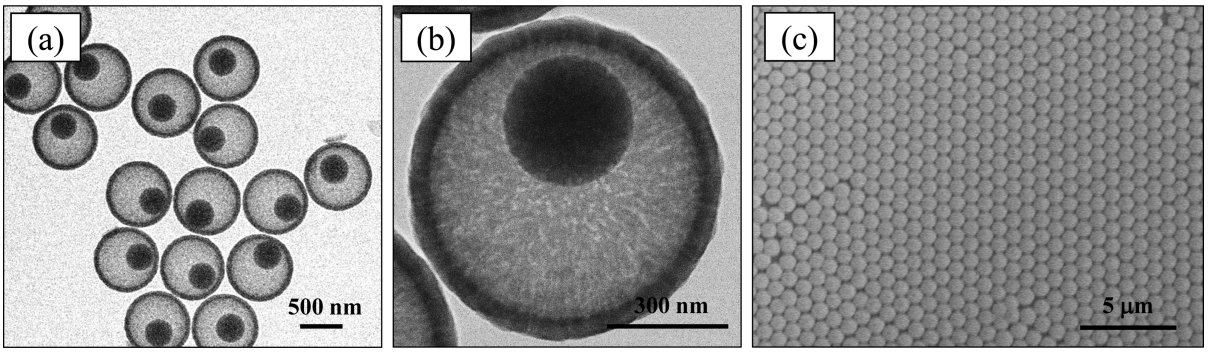

Figure 2. TEM images of yolk/shell particles incorporating a silica core with low (a) and high (b) magnifications, and SEM image (c) of an assembly of the yolk/shell particles.

shown in Figure S3e. The porosity of silica shell can be confirmed by the magnified image shown in Figure 2b. The size ratio of void space to cores of the yolk/shell particles (d_{void}/d_{core}) was around 2.2. The size distribution of yolk/shell particles was narrow with a C_V value of 2.2%. This was supported by the fact that they could be self-assembled as presented in Figure 2c, which shows the monolayered, quasi-hexagonal structures formed in a process where a droplet of the particle suspension was dried onto a substrate in air.

A tiny amount of water (approximately 20 μL) was dropped onto the dried particle assembly for observing the cores of yolk/shell particles in a wet state. Although no motions of cores were observed for the dried samples, more than 70% of the cores exhibited Brownian motion more than 15 min after immersing them into water (see Movie 1 in the Supporting Information). The Brownian motion of cores indicated that the water added to the dried samples could penetrate into porous silica shell. Figure 3 shows the traces of a movable core (A) and an immobile core (B) in the wet state. These locations of cores were tracked for 5 s and plotted in the figure with the origin of the coordinate axes for each core at $t = 0$. The axes normalized by average diameter of the cores are shown in the figure. Core (A) randomly moved in the ranges of $-0.1 < x < 0.4$ and $-0.2 < y < 0.3$, showing that it explored the space within the silica shell. On the other hand, the motion of core (B) was confined much more narrowly than that of core (A). Motions of other cores in the same assembly are presented in Figure S4.

To examine the motion of cores in response to an electric field, an external electric field was applied to the assembly of the yolk/shell particles. Figure 4 shows the traces of the cores with and without the field application. As shown in Figure 4, the

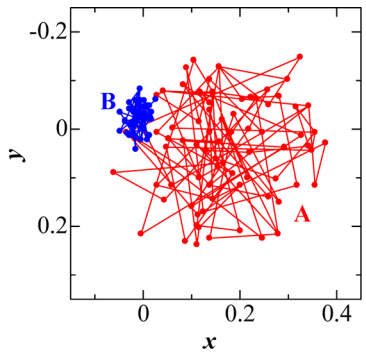

Figure 3. Representative traces of a movable particle (A, red) and an immobile particle (B, blue) incorporated into silica shell. The axes are normalized by the average dimeter of the core. The location y on the optical microscope image was inverted to show the core motions corresponding to Movie 1 in the Supporting Information.

core under the application of 1 MHz electric field with a strength of 100 V/mm randomly moved in the shell confinement, which is similar to that without the application of electric field (see Movie 2 in the Supporting Information).

A low-frequency electric field of 1 kHz was used to control the location of cores in the silica shell compartment. The application of a 1 kHz electric field with a strength of 50 V/mm seemed to restrict the cores to a plane orthogonal to the electric field as shown in Figure 5a. After switching the electric field off, the cores exhibited random Brownian motion again (see Movie 3 in the Supporting Information).

An increase in the electric field strength to 100 V/mm suppressed the anisotropic motion of cores even more and

DOI: 10.1021/acs.langmuir.6b03116
Langmuir 2017, 33, 296−302

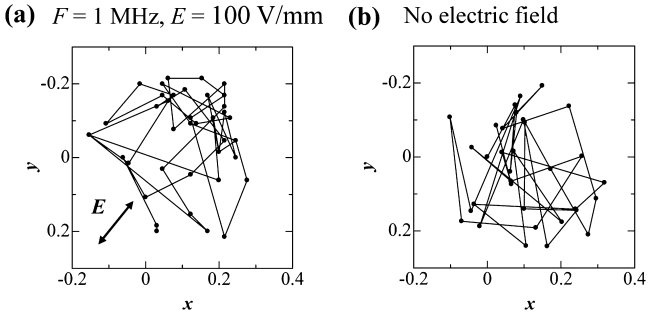

Figure 4. Traces of movable silica particles in the optical microscope images with the application of 1 MHz electric field at strength of 100 V/mm (a) and without the field application (b).

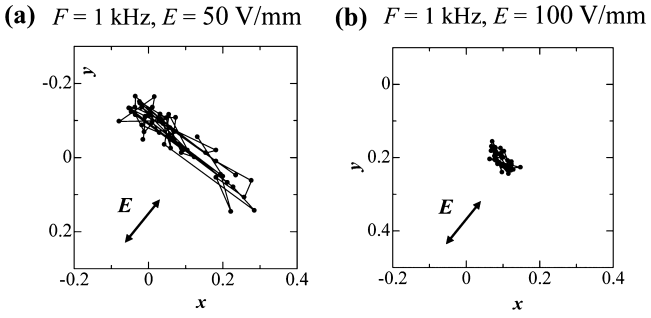

Figure 5. Traces of movable silica particles in the optical microscope images with the applications of 1 kHz electric field at strength of 50 V/mm (a) and 100 V/mm (b).

seemed to fix the cores at a specific location in the silica compartment. The suppression of core motion can be recognized in Figure 5b where the displacement of cores from the center of the hollow space was smaller than that observed at 50 V/mm of electric field. The mean square displacements (MSDs)[29] of cores traveling under three different applications of electric fields are shown in Figure S5. The characterizations indicated that the motion of inner core was confined by an increase in field strength at the low frequency of 1 kHz. Some different cores under the same applications of electric field were simultaneously observed with the optical microscope. As shown in Figure S6, it was confirmed that the motion of different cores were similar to each other in the same field application.

According to the results shown in Figures 4 and 5, a low-frequency (kHz) electric field was able to restrict the core motion and the ability to suppress the motion depended on the strength of electric field. Since application of a low-frequency field is able to perturb the electric double layer (EDL) covering the cores, the interaction between EDLs can play a pivotal role to induce the anisotropic motion of the cores in the shell.[30]

Figure 6a shows a TEM image of yolk/shell particles with a higher size ratio of hollow space to core compared with those shown in Figure 2. Their assembly fabricated by the self-assembled method is presented in Figure 6b. Similarly to Figure 5a, anisotropic motion of cores in these larger voids was still observed at 100 V/mm, which is higher than in the case of small hollow space. The anisotropic motion of the core in the large hollow space was strongly suppressed by a further increase in field strength to 150 V/mm at 0.5 kHz. Dependences of core motions on the void ratio, the electric field strength, and frequency are summarized in Table 1, where the observation results on silica cores incorporated into different hollow spaces are presented for various applied electric fields.

At zero field, all movable cores exhibited random Brownian motion in the shell compartment. A high-frequency electric field in the MHz range scarcely affected the location of silica cores with the void ratio of 3.0. In the case of low-frequency fields at 0.5 kHz, an increase in field strength to 50 V/mm restricted the random motion to exhibit anisotropic Brownian motion orthogonal to the electric field. An increase to 150 V/mm further suppressed the anisotropic motion and pinned the locations of cores almost at the centers of shell compartments.

A possible mechanism to explain the anisotropic motion of cores should include the deformation of EDLs surrounding the cores and shells because of the retardation effect operating in the direction of the electric field. Interaction between a core and its shell under application of electric field is schematically shown in Figure 7. In the case of low or null field strength, an EDL with a uniform thickness covers the surfaces of silica cores and shells (Figure 7a). An increase in field strength distorts the EDL thickness by stretching it in the field direction, as shown in Figure 7b. This restricts Brownian motion of the cores to a plane orthogonal to the electric field so as to minimize EDL overlap. A further increase in field strength stretches EDLs, leading to strong interaction and causing trapping of cores in the center due to strong repulsions between EDLs of core and shell.

This mechanism explains why suppressed motion is seen at lower field strength (at 0.5 and 1 kHz) for the particles with smaller voids. To check whether dielectric polarization could play a role in the described phenomena we prepared yolk/shell particles with cores made of a higher dielectric constant material. Figure 8 shows a TEM image of yolk/shell particles incorporating a titania core in a silica shell and a SEM image of their assembly fabricated by self-assembled method (see Figure

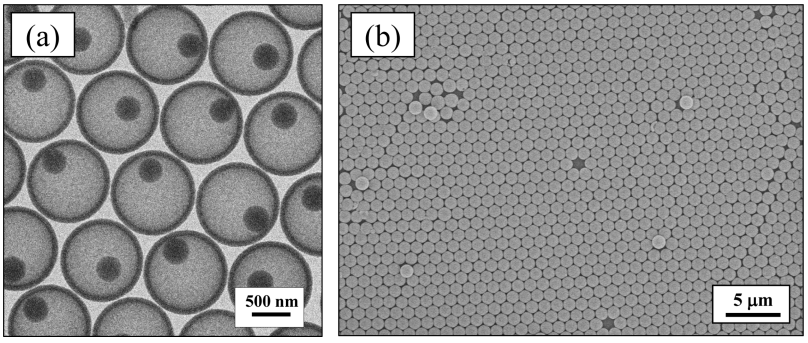

Figure 6. (a) TEM image of yolk/shell particles incorporating a silica core in a large void and (b) SEM image of the yolk/shell particle assembly.

DOI: 10.1021/acs.langmuir.6b03116
Langmuir 2017, 33, 296−302

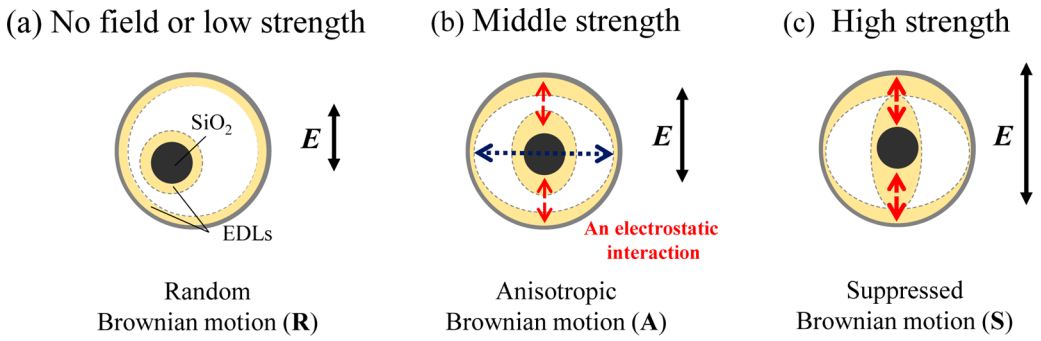

Figure 7. Schematic images of EDLs covering the cores and shells (d_{void}/d_{core} = 3.0) with 0 or low strength (a), middle strength (b), and high strength (c).

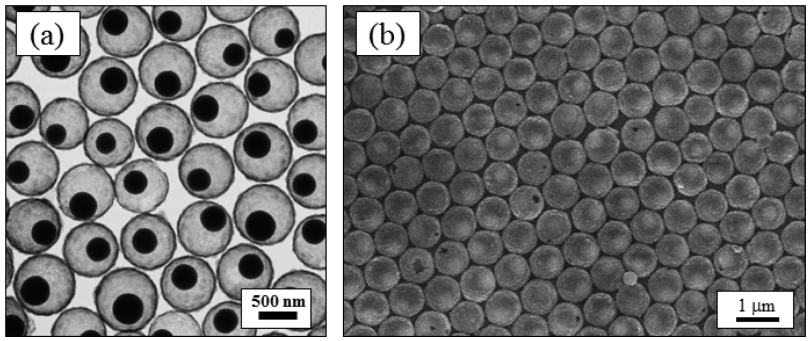

Figure 8. TEM image of rattle-type particles incorporating titania cores and SEM image of their assembly.

S7). Although the monodispersity of titania core was not high with C_V higher than 10%, that of yolk/shell particles finally obtained was sufficiently high to be regularly assembled (C_V around 6%). The void to core size ratio of these yolk/shell particles (d_{void}/d_{core}) was around 2.2, which is almost the same as that of the yolk/shell particles incorporating a silica core shown in Figure 2.

Titania cores incorporated into yolk/shell particles showed core motions different from silica cores. The difference in motion between titania and silica cores is summarized in Table 1.

Figure 9 shows the traces of titania cores under the application of electric field at a high-frequency of 1 MHz (a) and low-frequency of 1 kHz (b). As shown in Figure 9a, the cores were scarcely affected by the electric field at the high-frequency. At low-frequencies of 0.5 and 1.0 kHz, random Brownian motions were observed in the field strength range of 0−50 V/mm. An increase in field strength to 100 V/mm or higher caused anisotropic movement of the cores, as shown in Figure 9b (also see Movie 5 in the Supporting Information). Titania is known as a material more dielectric than silica in a wide frequency range.[31] If dielectric polarization were involved then a strong suppression of the titania core motion would be expected after application of an electric field. However, such a strong suppression was not observed. These results suggested that the bulk property of core permittivity was less dominant than interfacial properties of cores for controlling their location and motion. The surface potential of bare silica and titania particles after the combined process of heat treatment at 500 °C and etching were −41 and −17 mV, respectively. Therefore, the electrostatic interaction between EDLs of the silica core and the inner silica wall should be stronger than that between EDLs of the titania core and the silica shell as shown in Figure S8.

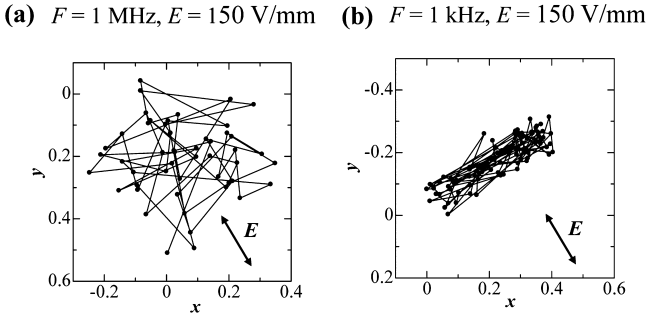

Figure 9. Traces of movable titania particles in the optical microscope images with the applications of electric field at the strength of 150 V/mm at 1 MHz (a) and 1 kHz (b).

CONCLUSION

Yolk/shell colloidal crystals incorporating movable cores were successfully fabricated by a combination of self-assembly and alkaline etching of yolk/shell particles. Approximately 70% of the cores were mobile in the shell compartment in water. Under the application of a 1 MHz electric field at strengths lower than 100 V/mm, the silica cores randomly moved in the shell confinement similarly to that without the application of electric field. In the case of low-frequency fields (kHz), however, the transition of the silica core motions could be controlled by the external electric fields. Under application of no or a low field strength, the cores exhibited random Brownian motion in the shell compartment. As electric field strength increased, the random motion became anisotropic or even suppressed Brownian motion altogether. Comparison of the core motions with those observed for yolk/shell particles with a large void space or with a titania core suggested that the motion of cores is mainly caused by field-induced changes in the

DOI: 10.1021/acs.langmuir.6b03116
Langmuir 2017, 33, 296−302

electrostatic interaction between the electric double layers of the core and the inner silica shell.

■ ASSOCIATED CONTENT

Supporting Information

The Supporting Information is available free of charge on the ACS Publications website at DOI: 10.1021/acs.langmuir.6b03116.

Detailed setup for electric field application and synthetic procedure for yolk/shell particles (PDF)

Brownian motion of cores in silica shell compartment, taken under 100× magnification (AVI, Movie 1)

Observation of the particle assembly under application of external electric fields at high-frequency of 1 MHz and strength of 100 V/mm (AVI, Movie 2)

Observation of the particle assembly at low-frequency of 1 kHz with strength of 50 V/mm (AVI, Movie 3)

Observation of the particle assembly at low-frequency of 1 kHz with strength 100 V/mm (AVI, Movie 4)

Motion of the titania cores under field application at 1 kHz and strength of 150 V/mm (AVI, Movie 5)

Movable and immobile particles incorporated into a silica shell, color coded in Figure S4 (AVI, Movie 6)

■ AUTHOR INFORMATION

Corresponding Author

*Tel: +81-22-795-7239. Fax: +81-22-795-7241. E-mail: dnagao@tohoku.ac.jp.

ORCID

Arnout Imhof: 0000-0002-7445-1360

Daisuke Nagao: 0000-0003-2710-5235

Notes

The authors declare no competing financial interest.

■ ACKNOWLEDGMENTS

This research was mainly supported by the Ministry of Education, Culture, Sports, Science and Technology (JSPS KAKENHI Grant Numbers 16J03375, 25600001, and 26286019).

■ ABBREVIATIONS

APTMS, 3-aminopropyltrimethoxysilane; *E*, electric field strength; EDL, electric double layer; *F*, frequency; KPS, potassium persulfate; MPTMS, 3-methacryloxypropyltrimethoxysilane; NaSS, *p*-styrenesulfonic acid sodium salt; NH_3, ammonia aqueous solution; PAH, poly(allylamine hydrochloride); PSt, polystyrene; PVP, polyvinylpyrrolidone; St, styrene; TEOS, tetraethyl orthosilicate; TTIP, titanium tetraisopropoxide

■ REFERENCES

(1) Galisteo-López, J.; Ibisate, M.; Sapienza, R.; Froufe-Pérez, L.; Blanco, A.; López, C. Self-Assembled Photonic Structures. *Adv. Mater.* **2011**, *23*, 30−69.

(2) Scheid, D.; Stock, D.; Gutmann, T.; Dietz, C.; Gallei, M. The Pivotal Step of Nanoparticle Functionalization of Functional and Magnetic Hybrid Opal Films. *J. Mater. Chem. C* **2016**, *4*, 2187−2196.

(3) Liu, X.; Zhang, Y.; Ge, D.; Zhao, J.; Li, Y.; Endres, F. Three-Dimensionally Ordered Macroporous Silicon Films Made by Electrodeposition from an Ionic Liquid. *Phys. Chem. Chem. Phys.* **2012**, *14*, 5100−5105.

(4) Alexeev, V. L.; Das, S.; Finegold, D. N.; Asher, S. A. Photonic Crystal Glucose-Sensing Material for Noninvasive Monitoring of Glucose in Tear Fluid. *Clin. Chem.* **2004**, *50*, 2353−2360.

(5) Zhang, J.-T.; Wang, L.; Lamont, D. N.; Velankar, S. S.; Asher, S. A. Fabrication of Large-Area Two-Dimensional Colloidal Crystals. *Angew. Chem., Int. Ed.* **2012**, *51*, 6117.

(6) Sharma, A. C.; Jana, T.; Kesavamoorthy, R.; Shi, L.; Virji, M. A.; Finegold, D. N.; Asher, S. A. A General Photonic Crystal Sensing Motif: Creatinine in Bodily Fluids. *J. Am. Chem. Soc.* **2004**, *126*, 2971−2977.

(7) Ge, J.; Lee, H.; Kim, J.; Lu, Z.; Kim, H.; Goebl, J.; Kwon, S.; Yin, Y. Magnetochromatic Microspheres: Rotating Photonic Crystals. *J. Am. Chem. Soc.* **2009**, *131*, 15687−15694.

(8) Lee, I.; Kim, D.; Kal, J.; Baek, H.; Kwak, D.; Go, D.; Kim, E.; Kang, C.; Chung, J.; Jang, Y.; Ji, S.; Joo, J.; Kang, Y. Quasi-Amorphous Colloidal Structures for Electrically Tunable Full-Color Photonic Pixels with Angle-Independency. *Adv. Mater.* **2010**, *22*, 4973−4977.

(9) Ge, J.; Kwon, S.; Yin, Y. Niche Applications of Magnetically Responsive Photonic Structures. *J. Mater. Chem.* **2010**, *20*, 5777−5784.

(10) He, L.; Wang, M.; Ge, J.; Yin, Y. Magnetic Assembly Route to Colloidal Responsive Photonic Nanostructures. *Acc. Chem. Res.* **2012**, *45*, 1431−1440.

(11) Weissman, J. M.; Sunkara, H. B.; Tse, A. S.; Asher, S. A. Thermally Switchable Periodicities and Diffraction from Mesoscopically Ordered Materials. *Science* **1996**, *274*, 959−963.

(12) Takeoka, Y.; Watanabe, M. Tuning Structural Color Changes of Porous Thermosensitive Gels through Quantitative Adjustment of the Cross-Linker in Pre-gel Solutions. *Langmuir* **2003**, *19*, 9104−9106.

(13) Tierno, P. Recent Advances in Anisotropic Magnetic Colloids: Realization, Assembly and Applications. *Phys. Chem. Chem. Phys.* **2014**, *16*, 23515−23528.

(14) Scheid, D.; Cherkashinin, G.; Ionescu, E.; Gallei, M. Signle-Source Magnetic Nanorattles By Using Conbenient Emulsion Polymerization Protocols. *Langmuir* **2014**, *30*, 1204−1209.

(15) Smoukov, S. K.; Gangwal, S.; Marquez, M.; Velev, O. D. Reconfigurable Responsive Structures Assembled from Magnetic Janus Particles. *Soft Matter* **2009**, *5*, 1285−1292.

(16) Tierno, P. Magnetically Reconfigurable Colloidal Patterns Arranged from Arrays of Self-Assembled Microscopic Dimers. *Soft Matter* **2012**, *8*, 11443−11446.

(17) Lee, S. H.; Liddell, C. M. Anisotropic Magnetic Colloids: A Strategy to Form Complex Structures Using Nonspherical Building Blocks. *Small* **2009**, *5*, 1957−1962.

(18) Hu, Y.; He, L.; Yin, Y. Magnetically Responsive Photonic Nanochains. *Angew. Chem., Int. Ed.* **2011**, *50*, 3747−3750.

(19) Sacanna, S.; Rossi, L.; Pine, D. J. Magnetic Click Colloidal Assembly. *J. Am. Chem. Soc.* **2012**, *134*, 6112−6115.

(20) Camargo, P. H. C.; Li, Z.; Xia, Y. Colloidal Building Blocks with potential for Magnetically Configurable Photonic Crystals. *Soft Matter* **2007**, *3*, 1215−1222.

(21) Okada, A.; Nagao, D.; Ueno, T.; Ishii, H.; Konno, M. Colloidal Polarization of Yolk/Shell Particles by Reconfiguration of Inner Cores Responsive to an External Magnetic Field. *Langmuir* **2013**, *29*, 9004−9009.

(22) Sakurai, Y.; Nagao, D.; Ishii, H.; Konno, M. Miniaturization of Anisotropic Composite Particles Incorporating a Silica Particle Smaller than 100 nm. *Colloid Polym. Sci.* **2014**, *292*, 449−454.

(23) Graf, C.; Vossen, D.; Imhof, A.; van Blaaderen, A. General Method To Coat Colloidal Particles with Silica. *Langmuir* **2003**, *19*, 6693−6700.

(24) Chen, D.; Li, L.; Tang, F.; Qi, S. Facile and Scalable Synthesis of Tailored Silica "Nanorattle" Structures. *Adv. Mater.* **2009**, *21*, 3804−3807.

(25) van Blaaderen, A.; Vrij, A. Synthesis and Characterization of Monodisperse Colloidal Organo-silica Spheres. *J. Colloid Interface Sci.* **1993**, *156*, 1−18.

(26) Mine, E.; Hirose, M.; Nagao, D.; Kobayashi, Y.; Konno, M. Synthesis of Submicrometer-Sized Titania Spherical Particles with a

Sol−Gel Method and Their Application to Colloidal Photonic Crystals. *J. Colloid Interface Sci.* **2005**, *291*, 162−168.
(27) Sugimoto, T.; Kojima, T. Formation Mechanism of Amorphous TiO_2 Spheres in Organic Solvents. 1. Roles of Ammonia. *J. Phys. Chem. C* **2008**, *112*, 18760−18771.
(28) Liu, J.; Qiao, S. Z.; Chen, S. J.; Lou, X. W.; Xing, X.; Lu, G. Q. Yolk/Shell Nanoparticles: New Platforms for Nanoreactors, Drug Delivery and Lithium-Ion Batteries. *Chem. Commun.* **2011**, *47*, 12578−12591.
(29) Wu, X.; Libchaber, A. Particle Diffusion in a Quasi-Two-Dimensional Bacterial Bath. *Phys. Rev. Lett.* **2000**, *84*, 3017−3020.
(30) Tsukahara, S.; Sakamoto, T.; Watarai, H. Positive Dielectrophoretic Mobilities of Single Microparticles Enhanced by the Dynamic Diffusion Cloud of Ions. *Langmuir* **2000**, *16*, 3866−3872.
(31) Zhang, L.; Zhang, H.; Wang, G.; Mo, C.; Zhang, Y. Dielectric Behaviour of Nano-TiO_2 Bulks. *Phys. Status Solidi* **1996**, *157*, 483−491.

DOI: 10.1021/acs.langmuir.6b03116
Langmuir 2017, 33, 296−302